ACS APPLIED MATERIALS & INTERFACES

Research Article

www.acsami.org

Improved Efficiency of Organic/Inorganic Hybrid Near-Infrared Light Upconverter by Device Optimization

Xinbo Chu, Min Guan,* Linsen Li, Yang Zhang, Feng Zhang, Yiyang Li, Zhanping Zhu, Baoqiang Wang, and Yiping Zeng*

Material Science Center, Institute of Semiconductors, Chinese Academy of Sciences, P.O. Box 912, Beijing, 100083, People's Republic of China

Supporting Information

ABSTRACT: An organic/inorganic hybrid up-conversion device was demonstrated in this work, which can convert near-infrared light (NIR) to visible green at high conversion efficiency. The upconverter was fabricated by integrating an $In_{0.12}Ga_{0.88}As/GaAs$ multiquantum wells (MQWs) photodetector (PD) with an organic light emitting diode (OLED). The up-conversion efficiency of 4.0 W/W % was obtained at 20 V under NIR illumination of 1mW/mm^2 at room temperature by optimizing the structure of the PD unit and adding MoO_3 doped perylene-3,4,9,10-tetracarboxylic dianhydride (PTCDA) as interfacial layer of OLED. Meanwhile, the green light output induced by NIR achieved 6050 cd/m^2, which proves that the organic/inorganic hybrid upconverter an excellent candidate that can be applied in light converter field.

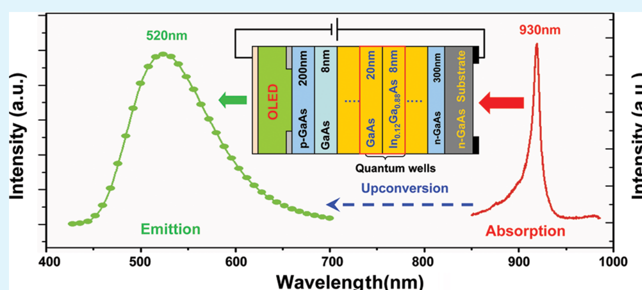

KEYWORDS: *hybrid up-conversion device, organic light-emitting diode, photodetector, near-infrared, MoO_3-doped PTCDA, interfacial layer*

INTRODUCTION

Optical up-conversion devices that can convert infrared light to visible light have been attracting increasing interests for their potential applications such as infrared imaging, night vision, and semiconductor wafer inspection.[1−6] Generally, the upconverters are integrated by a photo detector (PD) and a light-emitting diode (LED). Visible light is emitted out from the LED unit driven by the photocurrent, which is generated from the PD unit. Although monolithic integration of an inorganic PD and LED using epitaxial growth or wafer fusion has been demonstrated,[7−9] lattice matching requirement and band gap difference are still the main problems that restrict the up-conversion efficiency and response range of these devices.

Organic optoelectronic devices have been developed greatly and rapidly nowadays, especially organic light-emitting diodes (OLED), which has already been applied in solid state lighting and flat panel display fields.[10−13] Significant progress has been made by combining an OLED with an inorganic functional component due to the flexibility of depositing organic films on various substrates and relative simple processing.[14−16] In addition, OLED can work at ultralow temperature, which allows it with a great potential to be integrated with a long-wavelength infrared PD. Moreover, the emission wavelength of OLED can be easily tuned across visible region. Therefore, hybrid integration of an OLED with an inorganic PD can suitably combine the flexibility of organic semiconductors and high responsivity of inorganic PD together.

Significant progresses were reported by D. Ban et al. via integrating an OLED with an InGaAs/InP based p-i-n PD.[4,17,18] In our former work, up-conversion from wavelength of 980 to 520 nm was demonstrated with an efficiency of 0.81 W/W % by direct integration of an $In_{0.20}Ga_{0.80}As/GaAs$ MQWs PD and an OLED together.[19] The response wavelength of PD can be easily regulated in NIR region by changing indium content in wells. GaAs substrate also possesses an advantage of processing easily. Although MoO_3-doped CuPc was inserted between PD and OLED as an interfacial layer, dark current was still high, which led to a poor performance.[19] In this paper, we optimized the organic/inorganic hybrid device by PD unit and employing MoO_3 doped PTCDA as an interfacial connection layer. Incoming near-infrared (NIR) light was absorbed by the $In_{0.12}Ga_{0.88}As/GaAs$ based MQWs photodetector unit. And then the generated photocarriers were injected to the OLED component to emit green light. Thus, the interfacial layer between PD unit and OLED unit plays a critical role. At room temperature, the NIR induced green light output can reach 6050 cd/m^2, and the NIR to green up-conversion efficiency is 4.0W/W% at 20 V under a NIR illumination of 1mW/mm^2, which is five times higher than our former work, and it is also the best results ever reported that using p-i-n structure as photo detector without any internal gain effect.[17−19]

Received: July 16, 2012
Accepted: August 29, 2012
Published: August 29, 2012

 © 2012 American Chemical Society

■ EXPERIMENTAL SECTION

The inorganic epitaxial layers were grown in a VEECO GEN-II molecular beam epitaxy (MBE) system on n-GaAs substrate, consisting of 60 pairs $In_{0.12}Ga_{0.88}As$/GaAs MQWs as infrared absorption layer sandwiched between 300 nm n^+-GaAs ($3 \times 10^{18}cm^{-3}$, bottom) and 200 nm p^+-GaAs ($5 \times 10^{18}cm^{-3}$, top) layer. Figure 1 shows the cross-section schematic diagram of the organic–inorganic hybrid upconverter. The p type GaAs top layer was also as an anode contact of the OLED unit. Then 200 nm SiN_x film was deposited on the top surface of the PD unit as electrical isolation layer by using plasma-enhanced chemical vapor deposition (PECVD). Square windows were patterned using standard photolithography and etched onto the SiN_x layer using dry etching. Metal In was deposited on the back side of the PD unit, serving as the bottom contact for the upconverter.

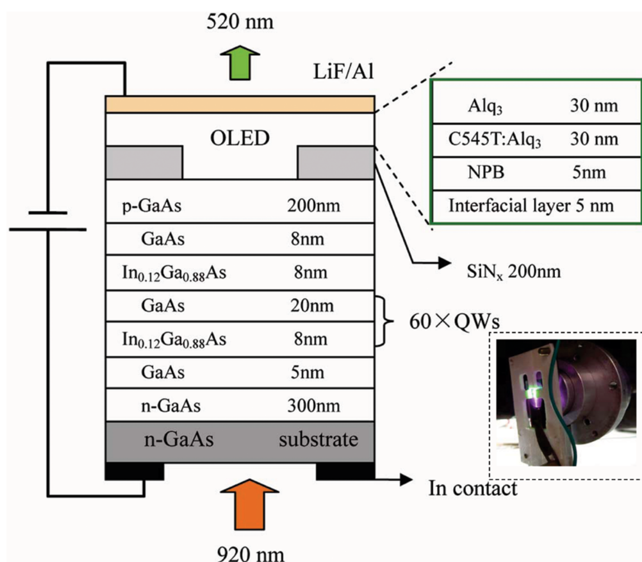

Figure 1. Cross-section schematic diagram of the organic−inorganic hybrid upconverter. The inset picture shows the NIR induced green light output from the hybrid upconverter.

The p-GaAs surface was boiled for 5 min in a mixture of sulfuric acid and phosphoric acid (H_2SO_4/H_3PO_4 = 3:1) to remove oxides and ultrasonic cleaned in ethanol, acetone for 5 min, respectively. Then, the sample was transferred into an organic molecular beam deposition system (OMBD) with a vacuum of 2×10^{-7} Torr for OLED layers deposition. Five nm thick PTCDA doped by MoO_3 was inserted between p-GaAs and *N,N′*-diphenyl-*N,N′*-bis(1,1′-biphenyl)-4,4′-diamine (NPB) as an interfacial layer to promote the photocarrier injection from PD to OLED unit. The organic stack consisted of NPB as hole transporting layer, 10-(2-benzo-thiazolyl)-2,3,6,7-tetrahydro-1,1,7,7-tetramethyl-1*H*,5*H*,11*H*-(1)-benzopyropyrano(6,7,8-*i,j*)-quinolizin-11-one:tris(8-hydroxyquinoline)aluminum ($C545T:Alq_3$) as emitting layer, and Alq_3 as electron transporting layer, respectively. LiF (1 nm)/Al (25 nm) semitransparent cathode was deposited on the top of the organic stack finally. The emission area of the devices was 1 mm^2 determined by the overlap area of the anode and the cathode. The hybrid upconverter was named as device A and previous device with SiO_2 layer as device B.

The current density−voltage−luminescence (*J*−*V*−*L*) characteristics of these devices were measured by a Keithley electrometer 2400 and a ST-86LA spot photometer. The emission spectra of the OLED units were measured by using a PR-650 Spectra Colorimeter. All measurements were carried out under ambient conditions without any protective coating. We also compared the performance of device A with the results of device B.[19] Both of them were fabricated and tested at the same condition except several structural differences, which were listed in Table 1.

Table 1. Several Structural Differences between Device A and Device B

device	insulating layer	periodicity	response wavelengh (nm)	interfacial layer
A	SiN_x	60	920	MoO_3:PTCDA
B	SiO_2	30	980	MoO_3:CuPc

■ RESULT AND DISCUSSIONS

Before the hybrid device fabrication, photoluminescence measurement was made to ensure the responding range of the PD component. As shown in Figure 2, the peak wavelength of the $In_{0.12}Ga_{0.88}As$ MQWs absorption layer located at 930 nm so that the 920 nm NIR laser was adopted as excitation light source. Figure 2 also presents the emission spectrum from OLED unit while the hybrid upconverter was in work. The peak wavelength of output emission spectrum was at 520 nm, which demonstrates the hybrid device can convert the NIR to green light.

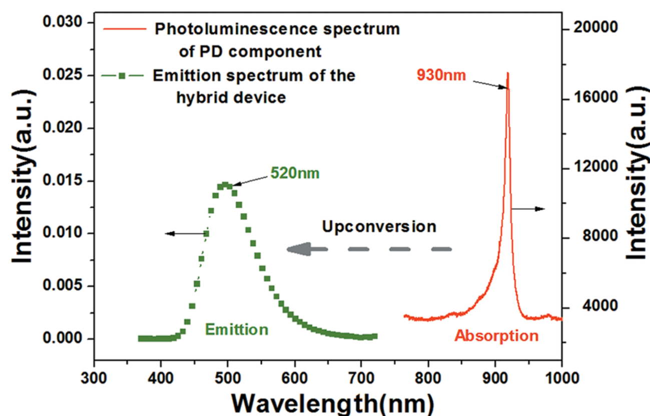

Figure 2. Photoluminescence spectrum of the PD component and emission spectrum of OLED unit when the hybrid upconverter is in work state.

The upconverter worked in a bias condition that the InGaAs/GaAs PD unit was under reverse bias and OLED under forward bias, as shown in Figure 1. The input NIR light was absorbed by the $In_{0.12}Ga_{0.88}As$/GaAs MQWs photodetector to generate photocarriers first, and then the photoinduced holes injected into organic layers of OLED component through the interfacial layer of MoO_3-doped PTCDA. The photoinduced holes combined with injected electrons from Al cathode in emitting layer, then the produced green light emitted from the top semitransparent cathode. The current density and luminance were measured under different NIR power density to demonstrate the up-conversion operation. The current density and luminance were very low under dark condition (no NIR input), as plotted in Figure 3. The turn-on voltage at 1.0 cd/m^2 was 3.7 V with a current density of 0.7 mA/cm^2. The current density and luminance at 20 V was just 134 mA/cm^2 and 1580 cd/m^2, respectively. The output luminance and total current density increased remarkably when the device was under NIR light illumination. For example, the turn on voltage dropped from 3.7 to 2.5 V and the output luminance achieved 7630 cd/m^2 under 1.0 mW/mm^2 illumination, which was nearly five times higher than that under dark condition. The current density also exhibited an obvious increase around 6 V, which indicates that the photocarriers injected from PD unit to

dx.doi.org/10.1021/am301340p | ACS Appl. Mater. Interfaces 2012, 4, 4976−4980

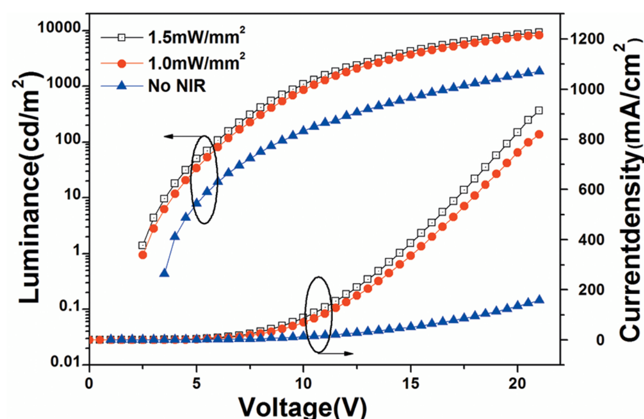

Figure 3. Output luminance and current density versus voltage under different irradiance power density.

transport layer of OLED efficiently. When the input power density of NIR increased from 1.0 mW/mm^2 to 1.5 mW/mm^2, the output luminance raised from 7630 cd/m^2 to 8400 cd/m^2 at 20 V, which also demonstrates that the hybrid device can convert NIR to visible light successfully at room temperature.

Optical power efficiency and responsivity of upconverter were calculated under 920 nm infrared radiation at 1.0mW/mm^2. Assuming that the upconverter in this work is a Lambertian source, the calculated optical power efficiency(W/A) equals luminance efficiency multiplied by π/488, in which 488 lm/W represents the effective power conversion constant that is normalized by the OLED emission spectrum (peaked in 520 nm). The photoresponsivity of the upconverter is calculated by dividing the photo current density (total current density plus dark current density) with power density of input NIR when the device was in work.[17,19] As is plotted in Figure 4a, the maximum of optical power efficiency was 0.01W/A at 3.5 V under 1.0mW/mm^2 illumination, then it decreased a fraction with the bias gradually increased. The responsivity rose at a low bias of 5 V and achieved the peak value of 6.1 A/W at 20 V. The overall up conversion efficiency can then be obtained by multiplying responsivity of upconverter (A/W) and optical power efficiency of OLED (W/A).[3,19] The up-conversion efficiency can reach 4.0 W/W% at 20 V, as shown in Figure 4b, which is 5 times higher than previous results (0.81 W/W %).

Unlike MoO_3:CuPc as an interfacial layer in device B, MoO_3:PTCDA was inserted between p-GaAs and NPB in device A instead. Figure 5 shows the calculated ratio of the dark current density versus the total current density while the device was under 1.0 mW/mm^2 NIR illumination. Although dry etching was used for device A to get square windows, which result in relatively rough surface, the ratio of device A is still much lower than device B especially at high bias, as shown in Figure 5. At the bias voltage of 10 V, the dark current ratio of device A is 17%, only about one-fourth of device B (66%), where the dark current density of device A is 12.7 mA/cm^2 and that of device B is 21.5 mA/cm^2. The ratio of device A achieved a plateau at 4.0 V. The high dark current of device B may originate from following two reasons. First, it is insufficient for the 30 periods of quantum wells as light absorption layer in photodetector unit of device B, which made the intrinsic layer too thin to absorb adequate photons. Thus photocarriers would be relatively low, which made the device B have a high dark current compared to device A. Second, because the upconverter was composed of photodetector unit tandem with OLED as a

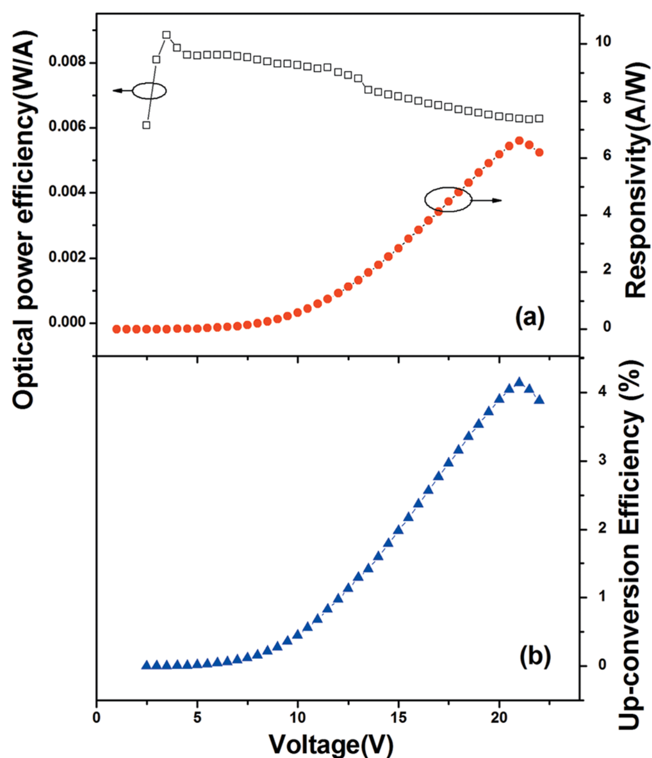

Figure 4. (a) Optical power efficiency and responsivity at different working bias. (b) Up-conversion efficiency versus voltage of device A under a NIR illumination of 1mW/mm^2.

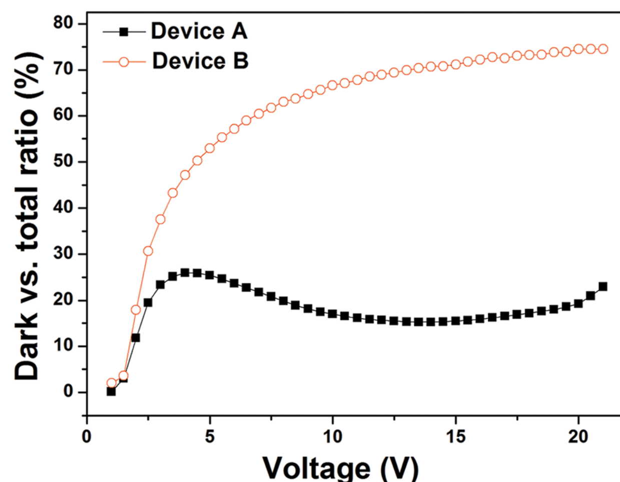

Figure 5. Calculated ratio of the dark current density versus the total current density of device A and device B when the device was under 1.0 mW/mm^2 NIR illumination.

whole, the current went across the interface and functional layers of OLED either. Thus, dark current density of the upconverter was also affected by the interfacial property and defects indwelling OLED layers. The plane PTCDA molecule may played a positive role in forming a smoother and more compact interfacial layer than CuPc on GaAs,[12] which reduced the density of micro pipes that may cause leakage current.

NIR induced green light outputs and responsivities were also compared between device A and device B. The responsivity of device A is 6.1A/W at 20 V, which is four times higher than that of device B, as shown in Figure 6a. It can be attributed to the doubled periodicity in MQWs layers from 30 to 60 pairs,

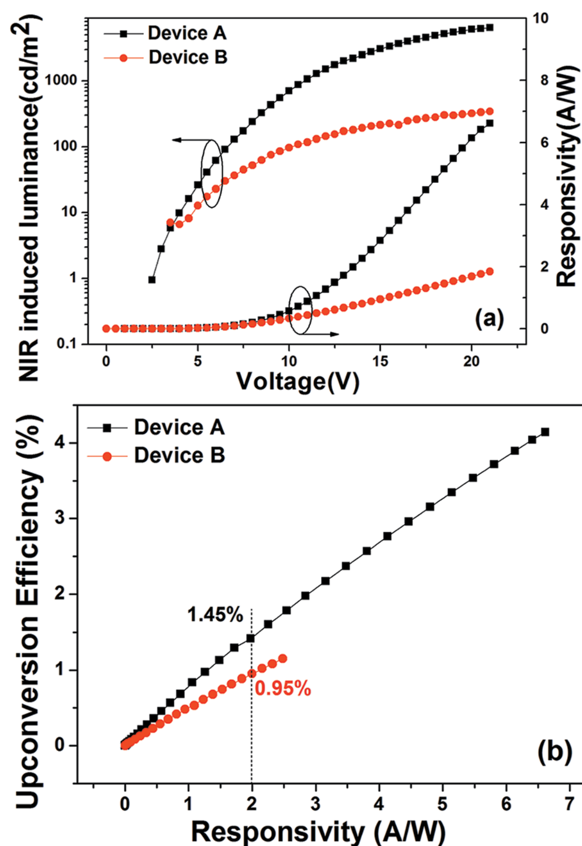

Figure 6. (a) NIR-induced luminance and responsivity of device A and B at different bias. (b) Up-conversion efficiency devices A and B under different responsivity.

which would promote more photos to be absorbed by the MQWs to generate more photocarriers. The NIR induced luminance of device A is 6050 cd/m^2 at 20 V, as shown in Figure 6a, which is much higher than 1260 cd/m^2 of device B. Device A had a NIR induced luminance of 2200 cd/m^2 at current density of 200 mA/cm^2, which was almost six times higher than that of device B (340 cd/m^2), further proving that a large proportion of current in device B does not pass through emitting layer adequately. NIR induced luminance of device A also increased more obviously, indicating that a relatively higher efficiency was obtained. It may originate from two factors as below. The PD unit of device A has a rather higher responsivity and generates more photocarriers than that of device B under the same NIR illumination. MoO_3 doped PTCDA as the interfacial layer between p-GaAs and NPB in device A have a better hole injection.

To further illustrate the critical role interfacial layer played, we compared the up-conversion efficiency under different responsivity to exclude the contribution from PD unit. As plotted in Figure 6b, the up-conversion efficiency is 1.45% for device A at responsivity of 2.0 A/W, improving by 50% compared to device B (0.95%). Up-conversion efficiency also linearly increases with the increase of responsivity. It clearly demonstrates that the layer of MoO_3:PTCDA has a better hole injection effect than that of MoO_3: CuPc when contacts with p-GaAs. The promotion of carrier injection can preliminary be attributed to the formation of charge transfer complex between MoO_3 and PTCDA that have been proved in our former work.[12] The charge transfer complex can improve hole concentration in connection layer for one thing and enhance electric conductivity for another.[20,21]

CONCLUSION

In summary, an NIR (920 nm) to green light (520 nm) optoelectronic up-conversion devices has been demonstrated at room temperature by direct tandem integration of an $In_{0.12}Ga_{0.88}As$/GaAs MQWs photodetector with an OLED. Through optimization of the PD unit and interfacial layer, the up-conversion efficiency achieved as high as 4.0%W/W at 20 V and a NIR induced luminance of 6050 cd/m^2 was obtained. The interfacial layer of MoO_3:PTCDA played a critical role in promoting photoinduced holes injection from p-GaAs to OLED effectively. This hybrid integration of an inorganic PD with an OLED as optical upconverter may open up new fields of infrared imaging and promote to understand the interfacial electrical property between organic semiconductors and inorganic materials. Therefore, in the following work, we will set out to improve the device performance from the aspect of improving the responsivity of PD unit and interface designing.

ASSOCIATED CONTENT

Supporting Information

The comparison of dark current density between device A and device B. This information is available free of charge via the Internet at http://pubs.acs.org.

AUTHOR INFORMATION

Corresponding Author

*Tel: +86-10-82304101 (M.G.); +86-10-82304657(Y.Z.). Fax: +86-10-82304232 (M.G.). E-mail: guanmin@semi.ac.cn (M.G.); ypzeng@semi.ac.cn (Y.Z.).

Notes

The authors declare no competing financial interest.

ACKNOWLEDGMENTS

The authors acknowledge the support of National Natural Science Foundation of China (NNSFC, Grants 61274049 and 61204012) and Beijing Natural Science Foundation (Grants 2123065 and 2112040).

REFERENCES

(1) Liu, H. C.; Gao, M.; Poole, P. *Electron. Lett.* **2000**, *36*, 1300–1301.
(2) Kim, D. Y.; Choudhury, K. R.; Lee, J. W.; Song, D. W.; Sarasqueta, G.; So, F. *Nano Lett.* **2011**, *11*, 2109–2113.
(3) Chen, J.; Ban, D.; Helander, M. G.; Lu, Z.-H.; Poole, P. *Adv. Mater.* **2010**, *22*, 4900–4904.
(4) Tao, J. C.; Chen, J.; Ban, D. Y.; Helander, M. G.; Lu, Z. H. *Sci. Adv. Mater.* **2012**, *4*, 266–281.
(5) Yang, Y.; Zhang, Y. H.; Shen, W. Z.; Liu, H. C. *Prog. Quant. Electron.* **2011**, *35*, 77–108.
(6) Chen, J.; Ban, D.; Helander, M. G.; Lu, Z.; Graf, M.; Poole, P.; Liu, H. *IEEE Photonics Technol. Lett.* **2009**, *21*, 1447–1449.
(7) Ban, D.; Luo, H.; Liu, H.; Wasilewski, Z.; Paltiel, Y.; Raizman, A.; Sher, A. *Appl. Phys. Lett.* **2005**, *86*, 201103.
(8) Liu, H. C.; Li, J.; Wasilewski, Z. R.; Buchanan, M. *Electron. Lett.* **1995**, *31*, 832–833.
(9) Yang, Y.; Shen, W.; Liu, H.; Laframboise, S.; Wicaksono, S.; Yoon, S.; Tan, K. *Appl. Phys. Lett.* **2009**, *94*, 093504.
(10) Forrest, S. R. *Nature* **2004**, *428*, 911–918.
(11) Li, X.; Chen, Z.; Zhao, Q.; Shen, L.; Li, F.; Yi, T.; Cao, Y.; Huang, C. *Inorg. Chem.* **2007**, *46*, 5518–5527.

(12) Li, L.; Guan, M.; Cao, G.; Li, Y.; Zeng, Y. *Appl. Phys. A: Mater. Sci. Process.* **2009**, *99*, 251−254.
(13) Yun, W. M.; Jang, J.; Nam, S.; Kim, L.; Seo, S. J.; Park, C. E. *ACS Appl. Mater. Interfaces* **2012**, *4*, 3247−3253.
(14) Heliotis, G.; Itskos, G.; Murray, R.; Dawson, M. D.; Watson, I. M.; Bradley, D. D. C. *Adv. Mater.* **2006**, *18*, 334−338.
(15) Bolink, H. J.; Brine, H.; Coronado, E.; Sessolo, M. *ACS Appl. Mater. Interfaces* **2010**, *2*, 2694−2698.
(16) Wehlus, T.; Korner, T.; Nowy, S.; Frischeisen, J.; Karl, H.; Stritzker, B.; Brutting, W. *Phys. Status Solidi A* **2011**, *208*, 264−275.
(17) Ban, D.; Han, S.; Lu, Z. H.; Oogarah, T.; SpringThorpe, A. J.; Liu, H. C. *Appl. Phys. Lett.* **2007**, *90*, 093108.
(18) Chen, J.; Ban, D.; Feng, X.; Lu, Z.; Fathololoumi, S.; SpringThorpe, A. J.; Liu, H. C. *J. Appl. Phys.* **2008**, *103*, 103112.
(19) Guan, M.; Li, L.; Cao, G.; Zhang, Y.; Wang, B.; Chu, X.; Zhu, Z.; Zeng, Y. *Org. Electron.* **2011**, *12*, 2090−2094.
(20) Mi, B. X.; Gao, Z. Q.; Cheah, K. W.; Chen, C. H. *Appl. Phys. Lett.* **2009**, *94*, No. 073507.
(21) Xie, G.; Meng, Y.; Wu, F.; Tao, C.; Zhang, D.; Liu, M.; Xue, Q.; Chen, W.; Zhao, Y. *Appl. Phys. Lett.* **2008**, *92*, No. 093305.